

Synthesis, characterization, and catalytic oxygenation activity of dinuclear iron(III) complex supported by binaphthol-containing chiral ligand

Takayuki Nagataki, Yoshimitsu Tachi, Shinobu Itoh*

^a Department of Chemistry, Graduate School of Science, Osaka City University, 3-3-138 Sugimoto, Sumiyoshi-ku, Osaka 558-8585, Japan

Received 12 July 2004; received in revised form 31 August 2004; accepted 31 August 2004

Available online 7 October 2004

Abstract

A diiron(III) complex supported by a new dinucleating ligand containing a chiral binaphthol spacer has been synthesized and characterized by elemental analysis and spectroscopic methods (ESI-MS, CD, and UV–vis). The complex has a (μ -oxo)(μ -carboxylato) doubly bridged diiron(III) core, the structural motif of which resembles that of the active site of sMMO and related diiron enzymes. Catalytic oxidation of alkanes with *m*-CPBA proceeded very efficiently to give the corresponding alcohols as the major products together with ketones as minor products. The alcohol-selectivity (alcohol/ketone = 3.8–8.8) as well as the kinetic deuterium isotope effect ($k_H/k_D = 3.0$ for the oxidation of cyclohexane) and significantly high regioselectivity (tertiary carbon/secondary carbon = 17.1) in the oxidation of adamantane strongly suggested a reaction mechanism involving a highly reactive metal-based oxidant rather than an autooxidation mechanism involving free radical species.

© 2004 Elsevier B.V. All rights reserved.

Keywords: Oxygenation; Alkane hydroxylation; Diiron complex; *m*-CPBA; Binaphthol

1. Introduction

Development of an efficient catalyst for selective oxygenation is an important objective in synthetic organic chemistry. Metalloenzymes accomplish highly efficient and selective oxygenation of organic molecules under very mild conditions, where molecular oxygen is mainly employed as the source of reactive intermediates [1–9]. Biomimetic studies have greatly contributed to characterization of the active oxygen intermediates involved in the enzymatic reactions and to understanding of their chemical reactivities and functions [10–17]. Recent advances in structural biology have also provided a great deal of information about mechanistic details of the enzymatic reactions [18], stimulating many synthetic chemists to design highly efficient catalysts for practical applications [10–13].

Recently, remarkable advances have been made in the chemistry of non-heme iron enzymes, especially, those with two proximal metal ions that yield novel active oxygen intermediates capable of performing diverse organic functionalizations [2,3,5,15]. A notable example is soluble methane monooxygenase (sMMO), in which a high-valent diiron-oxo species has been suggested to act as the key reactive intermediate for the alkane hydroxylation [2]. Significant insights into the dinuclear iron site not only of sMMO but also the related diiron enzymes have been attained through the synthetic modeling approach, whereby the detailed characterization of O₂ adducts or derived species provides fundamental spectroscopic, structural, and reactivity benchmarks for understanding the diiron active sites and, eventually, developing new oxidation catalysts [15,19].

In this study, we have designed a new dinucleating ligand LH₂ in order to replicate the structure and reactivity of the active sites of diiron enzymes. The ligand involves a binaphthol spacer to which *N,N*-bis(2-pyridylmethyl)aminomethyl group (Pym2) is attached at the 3- and 3'-positions (Fig. 1).

* Corresponding author. Tel.: +81 6 6605 2564; fax: +81 6 6605 2564.
E-mail address: shinobu@sci.osaka-cu.ac.jp (S. Itoh).

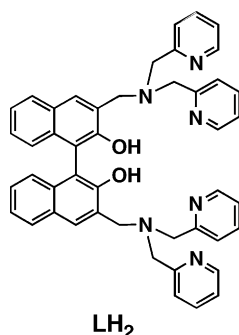


Fig. 1. Dinucleating ligand LH₂.

The Pym2 groups collaborate with the binaphthol group to provide an appropriate dinuclear metal binding site, where the binaphthol moiety is expected to work not only as a spacer to hold the Pym2 groups at a desirable distance but also as a chiral source for enantioselective oxidation. So far, a great deal of efforts have been made to develop non-heme iron catalysts for alkane hydroxylation, some of which have been demonstrated to produce a high-valent iron-oxo species as a reactive intermediate [20–22]. However, most of the catalysts so far been reported are those generated from mononuclear iron-complex precursors, whereas dinuclear iron catalysts supported by well-designed dinucleating ligands are very rare [23–25]. Moreover, there has been no report of a chiral dinuclear iron complex aiming for developing a catalyst for asymmetric hydroxylation [21].

2. Experimental

2.1. General

The reagents and the solvents used in this study except for the ligand and the complex were commercial products of the highest available purity and were further purified by the standard methods, if necessary [26]. Bis(2-pyridylmethyl)amine was prepared according to the reported procedure [27]. (*S*- and (*R*)-3,3'-Bis(chloromethyl)-2,2'-bis(methoxymethoxy)-1,1'-binaphthyl (**1**) was prepared from (*S*- and (*R*)-1,1'-bi-2-naphthol according to the reported procedures with a little modification [28]. FT-IR spectra were recorded with a Shimadzu FTIR-8200PC. Mass spectra were recorded with a JEOL JMS-700T Tandem MS station or a PE SCIEX API 150EX (for ESI-MS). ¹H NMR spectra were recorded on a JEOL LMN-ECP300WB or a LMX-GX400. ESR measurements were performed on a JEOL JES-ME spectrometer at –150 °C equipped with a variable temperature cell holder. UV–vis spectra were measured using a Hewlett-Packard HP8453 diode array spectrophotometer. CD spectra were recorded using a Jasco J-720W spectropolarimeter. Elemental analyses were performed on

a Perkin-Elmer or a Fisons instruments EA 1108 Elemental analyzer.

2.2. Synthesis of ligand

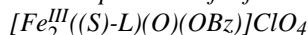
2.2.1. (*S*)-3,3'-Bis[*N,N*-bis(2-pyridylmethyl)aminomethyl]-2,2'-bis(methoxymethoxy)-1,1'-binaphthyl [(*S*)-L_{mom}]

Bis(2-pyridylmethyl)amine (Pym2) (0.86 g, 4.3 mmol), K₂CO₃ (0.96 g, 6.9 mmol), and dry CH₃CN (5 ml) were placed in a round bottom flask under N₂ atmosphere at room temperature. To this mixture, a CH₃CN solution (40 ml) of (*S*)-**1** (0.81 g, 1.7 mmol) was added dropwise under N₂ atmosphere over 30 min. After stirred for 44 h, insoluble materials were removed by filtration, and washed with CH₂Cl₂ several times until the washing solvent becomes colorless. The combined filtrate was concentrated, and the resulting residue was purified by alumina column chromatography by using ethyl acetate as an eluent to give a yellow oil (0.86 g, 62%). ¹H NMR (CDCl₃, 300 MHz): δ 2.68 (6 H, s, MOM–CH₃), 3.94 (4 H, d, *J* = 14.6 Hz, N–CH₂–Py), 4.00 (4 H, d, *J* = 14.6 Hz, N–CH₂–Py), 4.04 (2 H, d, *J* = 9.3 Hz, Ar–CH₂–N), 4.08 (2 H, d, *J* = 15.6 Hz, Ar–CH₂–N), 4.35 (2 H, d, *J* = 5.7 Hz, MOM–CH₂), 4.46 (2 H, d, *J* = 5.9 Hz, MOM–CH₂), 7.13–7.23 (8 H, m, Ar and Py), 7.38 (2 H, t, *J* = 7.3 Hz, Ar), 7.65–7.72 (8 H, m, Py), 7.89 (2 H, d, *J* = 8.0 Hz, Ar), 8.33 (2 H, s, Ar), 8.54 (4 H, dt, *J* = 4.8 Hz, 1.3 Hz, Py); IR (KBr): 1064 (C–N), 1147, 968 (MOM group), 1589, 1506, 754 cm^{–1} (aromatic); HR-MS (FAB⁺): *m/z* 797.3810 [*M* + H]⁺, calcd for C₅₀H₄₉N₆O₄ 797.3815. The (*R*)-isomer was prepared in the same way by using (*R*)-**1** instead of (*S*)-**1**.

2.2.2. (*S*)-3,3'-Bis[*N,N*-bis(2-pyridylmethyl)aminomethyl]-1,1'-bi-2-naphthol [(*S*)-LH₂]

To a THF solution (10 ml) of (*S*)-L_{mom} (591 mg, 0.74 mmol) was added 6N HCl (10 ml). Then, the mixture was stirred for 15 h at room temperature. After removal of the solvent under reduced pressure, the resulting residue was dissolved in water (30 ml) and the aqueous solution was treated with a saturated Na₂CO₃ aq. The mixture was extracted with CH₂Cl₂ (20 ml × 3), and the combined organic layer was washed with water and brine, and then dried over Na₂SO₄. After removal of Na₂SO₄ by filtration, evaporation of the solvent gave the title compound as a yellow oil (489 mg, 93%). ¹H NMR (CDCl₃, 400 MHz): δ 3.93 (4 H, d, *J* = 14.6 Hz, N–CH₂–Py), 3.97 (4 H, d, *J* = 14.6 Hz, N–CH₂–Py), 4.06 (2 H, d, *J* = 13.4 Hz, Ar–CH₂–N), 4.18 (2 H, d, *J* = 13.4 Hz, Ar–CH₂–N), 7.00–7.07 (6 H, m, Ar, Py), 7.15 (2 H, d, *J* = 8.1 Hz, Ar), 7.24 (2 H, t, *J* = 7.4 Hz, Ar), 7.36–7.44 (8 H, m, Py), 7.76 (2 H, s, Ar), 7.80 (2 H, d, *J* = 8.1 Hz, Ar), 8.41 (4 H, d, *J* = 4.9 Hz, Py), 10.74 (2 H, s br, ArOH); IR (KBr): 3062 (O–H), 1110 (C–N), 1635, 1436, 750 cm^{–1} (aromatic); HR-MS (FAB⁺): *m/z* 709.3300 [*M* + H]⁺, calcd for C₄₆H₄₁N₆O₂ 709.3291. The (*R*)-isomer was prepared in the same way by using (*R*)-L_{mom} instead of (*S*)-L_{mom}.

2.3. Preparation of diferric complex



A water solution (2 ml) of sodium benzoate (91 mg, 0.63 mmol) was added into an ethanol solution (3 ml) of $\text{Fe}^{\text{III}}\text{Cl}_3 \cdot 6\text{H}_2\text{O}$ (66 mg, 0.24 mmol) with stirring at room temperature. The mixture was turned to an orange suspension. After the mixture was stirred for 30 min, ligand (*S*)-LH₂ (50.0 mg, 0.07 mmol) was added into the mixture. The resulting mixture was further stirring for 2 h, during which the solution was turned to black. After adding NaClO_4 (87 mg, 0.71 mmol), the mixture was further stirred at room temperature for 24 h. The resulting black precipitates were collected by filtration, washed with water and ethanol, and dried (67.6 mg, 91%). IR (KBr): 1095 cm^{-1} (ClO_4); MS (ESI, positive): m/z 955.2 [$M - \text{ClO}_4$]⁺, calcd for $\text{C}_{53}\text{H}_{43}\text{N}_6\text{O}_5\text{Fe}_2$ 955.2; Anal. Calcd for $\text{C}_{53}\text{H}_{47}\text{N}_6\text{O}_{11}\text{Fe}_2\text{Cl} \cdot 2\text{H}_2\text{O}$: C, 58.34; H, 4.34; N, 7.70. Found: C, 57.97; H, 4.04; N, 7.31. The (*R*)-isomer was prepared in the same way by using (*R*)-LH₂ instead of (*S*)-LH₂.

2.4. Catalytic oxidation of hydrocarbons

Typically, the diiron(III) complex $[\text{Fe}_2^{\text{III}}((S)\text{-L})(\text{O})(\text{OBz})]\text{ClO}_4$ (2 μmol) in $\text{CH}_3\text{CN}-\text{CH}_2\text{Cl}_2$ (1:1 v/v) (2 ml) was added to a CH_2Cl_2 (2.4 ml) solution containing cyclohexane (15 mmol) and *m*-CPBA (2 mmol) under N_2 atmosphere with vigorous stirring at room temperature. The reaction mixture were analyzed with a Shimadzu GC-14A gas chromatograph equipped with a Restek Rtx-1701 capillary column (30 m \times 0.25 mm). All peaks of interest were identified by comparison of retention times and co-injection with authentic samples. The products were quantified by comparison against a known amount of internal standard using a calibration curve consisting of a plot of mole ratio (moles of organic compound/moles of internal standard) versus area ratio (area of organic compound/area of standard). In the case of tetralin as the substrate, the optical purity of the hydroxylated product was determined by using an HPLC system consisting of a Shimadzu LC-6A chromatographic pump and a Shimadzu UV-vis spectrophotometric detector SPD-6AV equipped with a chiral column (CHIRALCEL OB 250 mm \times 4.6 mm, Daicel Chemical Industries).

2.5. Determination of kinetic deuterium isotope effect

The diiron(III) complex $[\text{Fe}_2^{\text{III}}(\text{L})(\text{O})(\text{OBz})]\text{ClO}_4$ (2 μmol) in $\text{CH}_3\text{CN}-\text{CH}_2\text{Cl}_2$ (1:1 v/v) (2 ml) was added to a CH_2Cl_2 (2.4 ml) solution containing cyclohexane (0.81 ml, 7.5 mmol), cyclooctane (0.81 ml, 6.0 mmol), and *m*-CPBA (2 mmol) under N_2 atmosphere with vigorous stirring at room temperature. The oxidation products were analyzed by the GC method described above. The reaction was also carried out using cyclohexane-*d*₁₂ instead of cyclohexane.

The $k_{\text{H}}/k_{\text{D}}$ value for cyclohexanol was calculated by

$$\frac{(\text{moles of the products from cyclohexane})}{(\text{moles of the products from cyclooctane})} \cdot \frac{(\text{moles of the products from cyclohexane-}d_{12})}{(\text{moles of the products from cyclooctane})}$$

2.6. Determination of oxidant efficiency

After the catalytic reaction for 15 min, the reaction mixture was diluted with methanol to a total volume of 20 ml. The mole of remaining oxidant was determined by iodometric titration as follows. A portion (1.0 ml) of the diluted methanol solution was added to 1 M H_2SO_4 aqueous solution (20 ml) containing 1 mmol potassium iodide and a small amount of starch. The mixture turned brown due to generation of I_2 . Then, the mixture was titrated with 0.02 M $\text{Na}_2\text{S}_2\text{O}_3$ aqueous solution until the color disappeared.

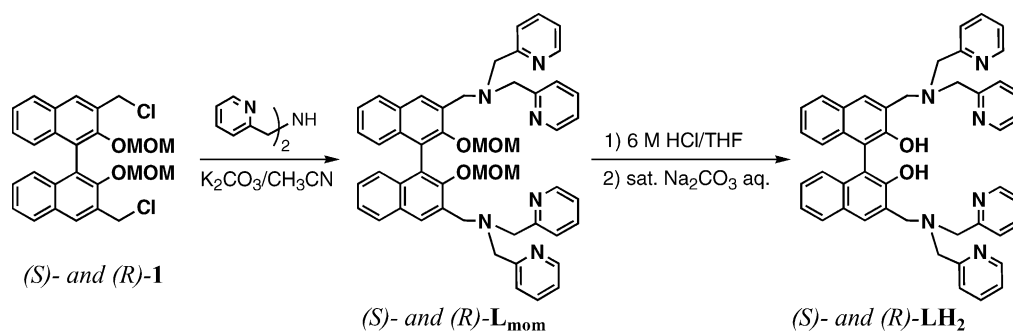
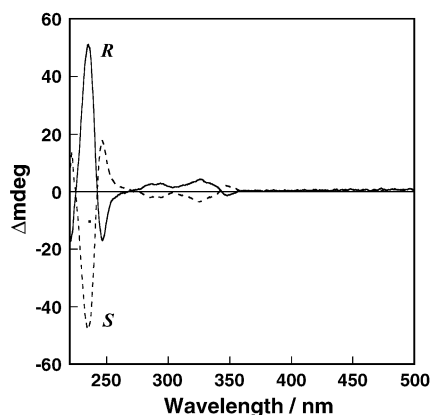
3. Results and discussion

3.1. Synthesis and characterization

Dinucleating ligand LH₂ was synthesized by the $\text{S}_{\text{N}}2$ reaction between bis(chloromethyl) binaphthol derivative **1** and bis(2-pyridylmethyl)amine followed by deprotection of the methoxymethyl (mom) groups as indicated in Scheme 1. The structure of LH₂ was well confirmed by ¹H NMR, IR, and HR-MS (see Section 2).

In Fig. 2 is shown the CD spectra of (*S*)- and (*R*)-LH₂ in CH_2Cl_2 at 25 °C. The CD spectrum of the (*S*)-isomer is the mirror image to that of the (*R*)-isomer with respect to the X-axis, confirming that the enantiomeric purity of the binaphthyl group is completely retained during the synthetic processes.

The optically pure diferric complexes [(*S*)- and (*R*)-derivatives] were synthesized by treating the ligands, (*S*)- and (*R*)-LH₂, and three-fold excess of ferric chloride hexahydrate in the presence of 9 equiv. of sodium benzoate in ethanol. Black powder was obtained after addition of sodium perchlorate into the final reaction mixture. In spite of our great efforts, any single crystals of the complex suitable for X-ray crystallographic analysis could not be obtained. However, the elemental analysis and the ESI-MS analysis shown in Fig. 3 unambiguously demonstrated that the complex was a diiron(III) complex containing (μ -oxo)(μ -carboxylato) bridges. Thus, an estimated structure of the diiron(III) complex is as illustrated in Fig. 4. The proposed structure of the diiron(III) complex was further supported by its UV-vis spectrum, which exhibits intense absorption bands at 340 nm ($\epsilon = 18400 \text{ M}^{-1} \text{ cm}^{-1}$; $9200 \text{ M}^{-1} \text{ cm}^{-1}/\text{Fe}$) and 590 nm ($6800 \text{ M}^{-1} \text{ cm}^{-1}$; $3400 \text{ M}^{-1} \text{ cm}^{-1}/\text{Fe}$) as shown in Fig. 5. The spectral shape and the peak positions of the present complex are very close to those of the

Scheme 1. Synthesis of ligand LH₂.Fig. 2. CD spectra of (*R*)-LH₂ (solid line) and (*S*)-LH₂ (dotted line) (1.0×10^{-4} M) in CH₂Cl₂ at 25 °C.

diiron(III)–diphenolate complex containing (μ -oxo) and (μ -carboxylato) bridges reported by Que and coworkers [336 nm ($\epsilon = 8900 \text{ M}^{-1} \text{ cm}^{-1}/\text{Fe}$) and 522 nm ($3300 \text{ M}^{-1} \text{ cm}^{-1}/\text{Fe}$) [29]. The lower energy band was assigned to a phenolate-to-Fe(III) charge transfer transition and the higher energy band has been attributed to both phenolate- and oxo-to-Fe(III) charge transfer transitions [29]. The complex was ESR-silent, presumably due to a strong antiferromagnetic interaction between the two ferric ions, the magnetic property of which

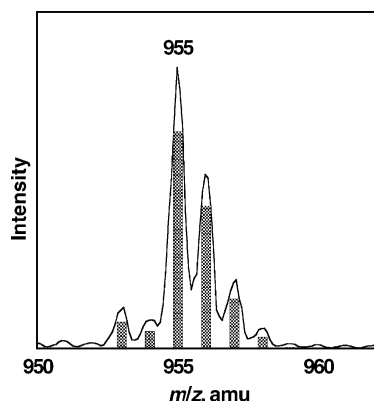
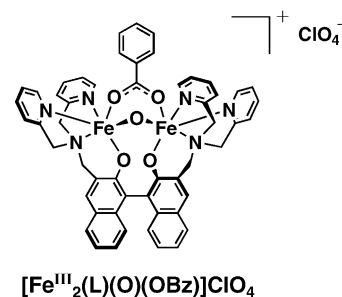
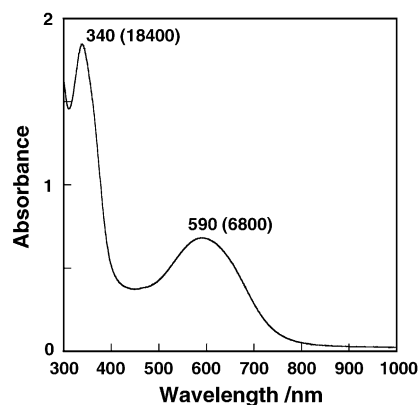
Fig. 3. ESI-MS spectrum of $[\text{Fe}_2(\text{L})(\text{O})(\text{OBz})]\text{ClO}_4$. The solid line shows the observed spectrum. The bars represent the isotope distribution calculated for $[\text{C}_{53}\text{H}_{43}\text{N}_6\text{O}_5\text{Fe}_2]^+$.

Fig. 4. Estimated structure of the diiron(III) complex.

was also similar to that of the Que's complex [29]. In Fig. 6 are shown the CD spectra of the (*S*)- and (*R*)-isomers of the diiron(III) complex in CH₃CN. The spectra of (*S*)- and (*R*)-isomers are also completely mirror image each other with respect to the X-axis, demonstrating that the optical purity was maintained during the complex formation process.

3.2. Catalytic oxygenation of alkanes

As demonstrated above, the complex has a (μ -oxo)(μ -carboxylato) doubly bridged diiron(III) core, the structural motif of which resembles that of the active sites of sMMO and related enzymes [2,3]. Thus, catalytic activity of the diiron(III) complex was examined in the oxygenation reaction

Fig. 5. UV-vis spectrum of $[\text{Fe}_2(\text{L})(\text{O})(\text{OBz})]\text{ClO}_4$ (1.0×10^{-4} M) in CH₃CN at 25 °C.

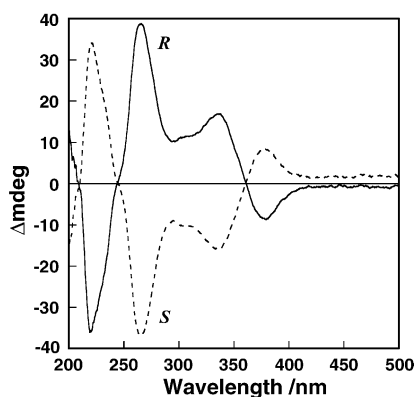


Fig. 6. CD spectra of (*R*)-[Fe₂(L)(O)(OBz)]ClO₄ (solid line) and (*S*)-[Fe₂(L)(O)(OBz)]ClO₄ (dotted line) (1.0×10^{-4} M) in CH₃CN at 25 °C.

of alkanes as summarized in Table 1. In the reaction of cyclohexane, oxidation with *m*-CPBA (*m*-chloroperoxybenzoic acid) proceeded catalytically to give cyclohexanol as the major product together with cyclohexanone as a minor product, where the product ratio of alcohol/ketone (A/K) was 6.5. The total turnover number (TON = moles of products/moles of catalyst) of the catalyst reached 270 within 15 min, and the oxidant efficiency (moles of product/moles of *m*-CPBA consumed after the reaction) was 61% (see Section 2). Furthermore, an appreciable amount of kinetic deuterium isotope effect ($k_{\text{H}}/k_{\text{D}} = 3.0$) was obtained when cyclohexane-*d*₁₂ was employed as the substrate (see Section 2). On the other hand, the reaction with other oxidants such as TBHP (*t*-BuOOH) and H₂O₂ gave much lower TON and lower A/K values (1–1.7) (see Table 1), suggesting that the reac-

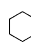
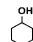
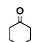
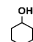
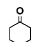
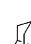
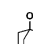

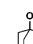

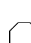
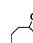
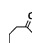


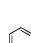
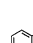
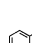
tion mechanism of the former is different from that of the later.

Oxidation of adamantane with *m*-CPBA also proceeded efficiently with a high TON (172.8) to give the corresponding alcohols together with a small amount of ketone. In this case as well, TBHP and H₂O₂ were poorer oxidants. It should be noted that the regioselectivity between secondary (2°) and tertiary (3°) carbons was quite high as 17.1 (the value derived from the amount of 1-adamantanol divided by the amounts of 2-adamantanol and 2-adamantanone and multiplied by 3 to correct for the higher number of secondary C–H bonds).

The catalytic activity of the diferric complex was further examined using cyclooctane, ethylbenzene, and tetralin as the substrates and *m*-CPBA as the oxidant (Table 1). In all the cases, the corresponding alcohols were obtained as the major products together with the corresponding ketones as the minor products with A/K ratio = 3.8–8.8. The difference in apparent TON among the substrates can be attributed in part to the difference in the number of C–H bonds to be oxidized. Thus, the TONs normalized just for one C–H bond of the substrates were rather constant (22.5 for cyclohexane, 24.3 for cyclooctane, 19.0 for ethylbenzene, and 24.5 for tetralin) except for adamantane (36.8 for 3°-carbon and 10.8 for 2°-carbon).

The enantioselectivity in the *m*-CPBA-oxidation was tested by using tetralin as the substrate and the (*S*)-isomer complex as the catalyst under otherwise the same experimental conditions. Enantiomeric excess (*ee*) of the product was determined by HPLC with a chiral column (see, Section 2). Unfortunately, however, the *ee* value was unexpectedly low (~10%; (*R*)-isomer was the major product of alcohol).

Table 1
Catalytic oxidation of alkanes by [Fe^{III}(L)(O)(OBz)]ClO₄^a

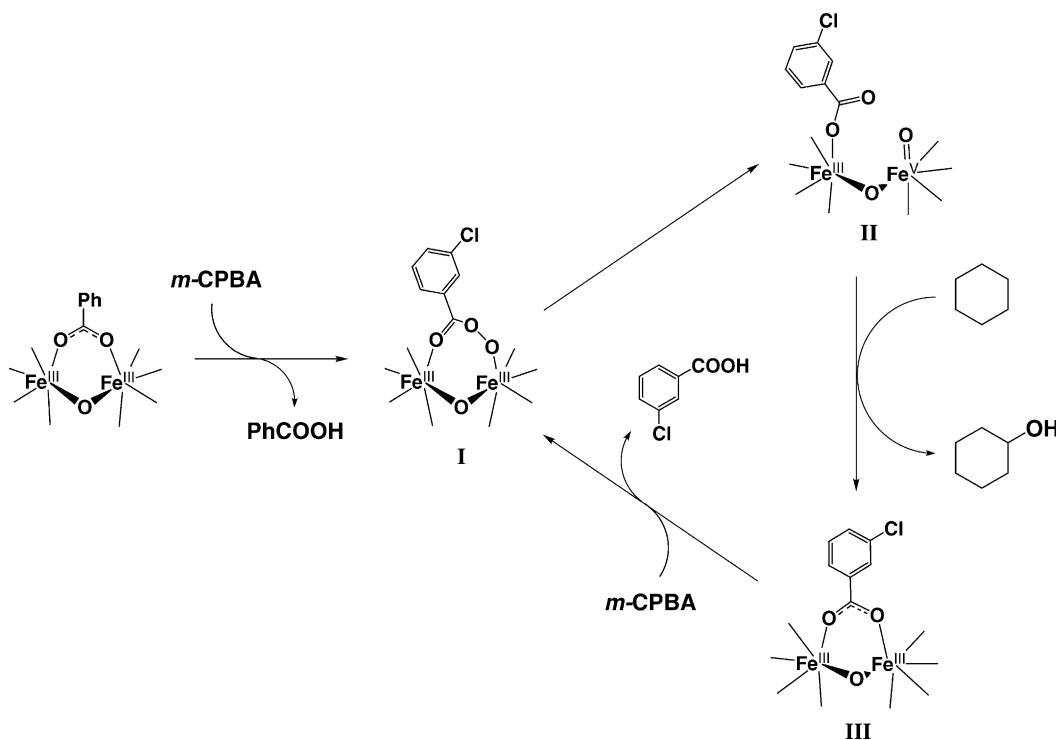
Substrate	Oxidant	Time	Products and TON ^b			
	<i>m</i> -CPBA	15 min		234		36 ^c
	TBHP	24 h		9.1		5.4
	H ₂ O ₂	24 h		3.2		3.4
 ^d	<i>m</i> -CPBA	15 min		147		20
	TBHP	24 h		6.0		1.1
	H ₂ O ₂	24 h		5.2		1.6
	<i>m</i> -CPBA	15 min		341		48
	<i>m</i> -CPBA	15 min		30		8.0
	<i>m</i> -CPBA	15 min		88 (9.9% <i>ee</i>)		10

^a Reaction conditions: [catalyst] = 0.33 mM; [oxidant] = 0.24 M; [substrate] = 2.5 M in CH₂Cl₂/CH₃CN at room temperature.

^b Turnover number (moles of product/moles of catalyst) determined by GC using calibration curves of the products.

^c A trace amount of ϵ -caprolactone was formed.

^d The reaction was carried out under diluted conditions because of the low solubility of adamantane in the solvents: [catalyst] = 0.17 mM; [oxidant] = 61 mM; [substrate] = 0.33 M.



Scheme 2. Proposed mechanism for the alkane hydroxylation.

3.3. Mechanistic consideration

Attempts to detect any intermediates derived from the reaction of the diiron(III) complex and *m*-CPBA have been unsuccessful. Namely, no spectral change was observed at a low temperature ($-40\text{ }^{\circ}\text{C}$), whereas raising the temperature to room temperature only resulted in decomposition of the catalyst in the absence of the substrate. Nonetheless, the observed KIE ($k_{\text{H}}/k_{\text{D}} = 3.0$) and the significantly large regioselectivity (tertiary carbon/secondary carbon = 17.1) in the adamantane oxidation, as well as the large A/K ratio strongly suggested a reaction mechanism involving a highly reactive metal-based oxidant rather than an autooxidation mechanism involving free radical species [21,22].

One of the possible reaction pathways of the catalytic oxygenation reaction is shown in Scheme 2. Ligand exchange between the benzoate bridging ligand and *m*-CPBA may take place to give a peracid-diiron(III) intermediate I, from which a Fe(III)–O–Fe(V)=O type intermediate II may be formed via heterolytic cleavage of the O–O bond. The high valent iron oxo species may oxidize the substrate via hydrogen atom abstraction and subsequent oxygen rebound mechanism or its concerted variant as proposed in the related model reactions and the sMMO reaction [3,22]. The resulting Fe(III)–O–Fe(III) species III may react with another molecule of *m*-CPBA to regenerate the intermediate I, completing the catalytic cycle. In support of this mechanism, addition of sodium benzoate (50 equiv. of the catalyst) into the reaction mixture enhanced the oxygenation reaction of cyclohexane (TON = 369, oxidant efficiency = 85%). In this

case, sodium benzoate may act as a base to enhance deprotonation of *m*-CPBA, accelerating the ligand exchange reaction (Scheme 2).

Although a high turnover number of diferric complex was attained in the initial stage of the *m*-CPBA-oxidation of alkanes, the catalytic activity was almost lost within 15 min as shown in Fig. 7. In order to get information about the degradation product of catalyst, the reaction mixture was analyzed by ESI-MS (Fig. 8). There was a prominent peak at $m/z = 656$, the peak position and the isotope distribution pattern of which were consistent with the chemical structure of the decomposition product IV (inset in Fig. 8). Thus, the self-oxidation

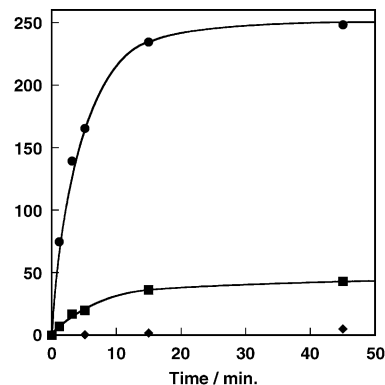


Fig. 7. Time courses for the formation of products in the oxidation of cyclohexane with *m*-CPBA catalyzed by $[\text{Fe}_2(\text{L})(\text{O})(\text{OBz})]\text{ClO}_4$ in $\text{CH}_2\text{Cl}_2/\text{CH}_3\text{CN}$ at $25\text{ }^{\circ}\text{C}$. Products: cyclohexanol (●), cyclohexanone (■), and ϵ -caprolactone (◆).

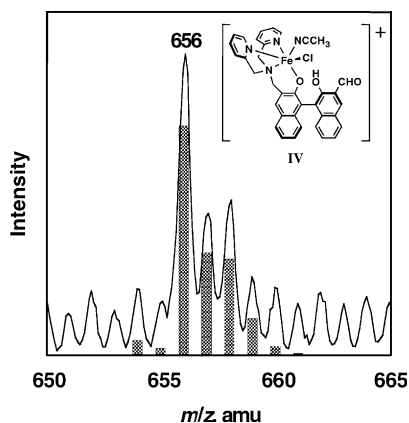


Fig. 8. ESI-MS spectrum of the degradation product of $[\text{Fe}_2(\text{L})(\text{O})(\text{OBz})]\text{ClO}_4$. The solid line shows the observed spectrum. The bars represent the isotope distribution calculated for $[\text{C}_{36}\text{H}_{29}\text{N}_4\text{O}_3\text{FeCl}]^+$.

at the benzylic position of the ligand sidearm might occur to induce the catalyst-degradation.

In summary, a dinuclear iron(III) complex has been synthesized using a new chiral dinucleating ligands LH_2 . As we expected, the ligand supports two ferric ions in an appropriate position to give the dinuclear iron(III) complex with $(\mu\text{-oxo})(\mu\text{-carboxylato})$ bridges, the structural motif of which is close to that of non-heme diiron metalloenzymes. The axial chirality of the binaphthyl moiety was maintained throughout the ligand synthesis and the complex formation. A significantly high catalytic activity of the diferric complex was obtained in the oxidation of a series of alkanes with *m*-CPBA, where formation of a high valent iron-oxo species has been suggested by the high alcohol-selectivity as well as the KIE (kinetic deuterium isotope effect) and significantly high regioselectivity (tertiary carbon vs. secondary carbon) in the adamantane oxidation. However, the enantioselectivity and the stability of catalyst were not satisfactory. Thus, rational ligand design will be further needed to enhance the stereoselectivity and stability of the catalysts.

Acknowledgments

This work was financially supported in part by Grant-in-Aid for Scientific Research on Priority Area (No. 11228206), Grant-in-Aid for Scientific Research (Nos. 13480189 and 15350105), and Grant-in-Aid for Young Scientists (B) (No. 14740368) from the Ministry of Education, Culture, Sports, Science and Technology, Japan. The authors also thank Prof.

Isamu Kinoshita of Osaka City University for his help in obtaining the CD spectra.

References

- [1] J.S. Valentine, C.S. Foote, A. Greenberg, J.F. Liebman (Eds.), *Active Oxygen in Biochemistry*, Chapman & Hall, London, 1995.
- [2] M. Merckx, D.A. Kopp, M.H. Sazinsky, J.L. Blazyk, J. Müller, S.J. Lippard, *Angew. Chem. Int. Ed.* 40 (2001) 2782.
- [3] M.-H. Baik, M. Newcomb, R.A. Friesner, S.J. Lippard, *Chem. Rev.* 103 (2003) 2385.
- [4] L. Que Jr., R.Y.N. Ho, *Chem. Rev.* 96 (1996) 2607.
- [5] B.J. Wallar, J.D. Lipscomb, *Chem. Rev.* 96 (1996) 2625.
- [6] E.I. Solomon, U.M. Sundaram, T.E. Machonkin, *Chem. Rev.* 96 (1996) 2563.
- [7] J.P. Klinman, *Chem. Rev.* 96 (1996) 2541.
- [8] T.J. Kappock, J.P. Caradonna, *Chem. Rev.* 96 (1996) 2659.
- [9] M. Sono, M.P. Roach, E.D. Coulter, J.H. Dawson, *Chem. Rev.* 96 (1996) 2841.
- [10] T. Funabiki (Ed.), *Oxygenases and Model Systems*, Kluwer Academic Publishers, Dordrecht, 1997.
- [11] B. Meunier (Ed.), *Biomimetic Oxidations Catalyzed by Transition Metal Complexes*, Imperial College Press, London, 1999.
- [12] B. Meunier (Ed.), *Metal-oxo and Metal-peroxo Species in Catalytic Oxidations*, Springer, Berlin, 2000.
- [13] L.I. Simándi (Ed.), *Advances in Catalytic Activation of Dioxygen by Metal Complexes*, Kluwer Academic Publishers, Dordrecht, 2003.
- [14] M. Costas, M.P. Mehn, M.P. Jensen, L. Que Jr., *Chem. Rev.* 104 (2004) 939.
- [15] E.Y. Tshuva, S.J. Lippard, *Chem. Rev.* 104 (2004) 987.
- [16] L.M. Mirica, X. Ottenwaelder, T.D.P. Stack, *Chem. Rev.* 104 (2004) 1013.
- [17] E.A. Lewis, W.B. Tolman, *Chem. Rev.* 104 (2004) 1047.
- [18] A. Messerschmidt, R. Huber, T. Poulos, K. Wieghardt (Eds.), *Handbook of Metalloproteins*, vols. 1 and 2, Wiley, Chichester, 2001.
- [19] L. Que Jr., W.B. Tolman, *Angew. Chem. Int. Ed.* 41 (2002) 1114.
- [20] D.H.R. Barton, D. Doller, *Acc. Chem. Res.* 25 (1992) 504.
- [21] M. Fontecave, S. Ménage, C. Duboc-Toia, *Coord. Chem. Rev.* 178–180 (1998) 1555.
- [22] M. Costas, K. Chen, L. Que Jr., *Coord. Chem. Rev.* 200–202 (2000) 517.
- [23] Y. Dong, S. Yan, V.G. Young Jr., L. Que Jr., *Angew. Chem. Int. Ed. Engl.* 35 (1996) 618.
- [24] T. Ookubo, H. Sugimoto, T. Nagayama, H. Masuda, T. Sato, K. Tanaka, Y. Maeda, H. Okawa, Y. Hayashi, A. Uehara, M. Suzuki, *J. Am. Chem. Soc.* 118 (1996) 701.
- [25] M. Kodera, H. Shimakoshi, K. Kano, *Chem. Commun.* (1996) 1737.
- [26] W.L.F. Armarego, D.D. Perrin, *Purification of Laboratory Chemicals*, 4th ed., Butterworths/Heinemann, Oxford, 1996.
- [27] D.W. Gruenwedel, *Inorg. Chem.* 7 (1968) 495.
- [28] F. Tani, M. Matsu-ura, S. Nakayama, M. Ichimura, N. Nakamura, Y. Naruta, *J. Am. Chem. Soc.* 123 (2001) 1133.
- [29] S. Yan, L. Que Jr., L.F. Taylor, O.P. Anderson, *J. Am. Chem. Soc.* 110 (1988) 5222.